PCCP

Accepted Manuscript

Volume 1 | Number 1 | Jan 2013 | Pages 1–100

PCCP

Physical Chemistry Chemical Physics

www.rsc.org/pccp

ROYAL SOCIETY OF CHEMISTRY

ROYAL SOCIETY
OF CHEMISTRY

www.rsc.org/pccp

PCCP

COMMUNICATION

Ultrafast excited state hydrogen atom transfer in salicylideneaniline driven by changes in aromaticity

Received 26th June 2015,
Accepted 00th January 20xx

DOI: 10.1039/x0xx00000x

www.rsc.org/

Luis Gutiérrez-Arzaluz,[a] Fernando Cortés-Guzmán,[a] Tomás Rocha-Rinza*[a] and Jorge Peón[a]

We investigated two important unresolved issues on excited state intramolecular proton transfer (ESIPT) reactions, i.e., their driving force and the charge state of the transferred species by means of quantum chemical topology. We related changes in the aromaticity of a molecule after electron excitation to reaction dynamics in an excited state. Additionally, we found that the conveyed particle has a charge intermediate between that of a bare proton and a neutral hydrogen atom. We anticipate that the analysis presented in this communication will yield valuable insights about ESIPT and other similar photochemical reactions.

Excited state intramolecular proton transfer (ESIPT) processes[1,2] are important photochemical reactions that illustrate the considerable change in the chemical properties of a molecule, e.g. the relative stability of its different tautomers that might occur after electron excitation. Many different and diverse systems exhibit ESIPT, leading to a considerable interest in this phenomenon.[1,3–8] The study of ESIPT transitions has led to the development of several technological applications such as molecular sensors,[1,9] white-light emitting materials,[1] fluorescent molecular and biological probes,[1,10] or optoelectronic devices.[11] This technology is based on the possibility to modulate distinct features of ESIPT processes like emission and absorption wavelengths, reaction reversibility or the affinity for a specific group in molecules interacting with the proton transfer system.[1–3,5,6,11,12]

The Schiff base salicylideneaniline (SA) is an interesting system to study ESIPT due to its unusual excited state dynamics in comparison with analogous compounds.[10,13–18] Scheme 1 shows the ESIPT process in SA. After the molecule is excited by light corresponding to the first electronic transition of the enol form, the tautomerism reaction takes place in the excited state, forming in this way a keto isomer which then may evolve into different conformers. The photo-induced proton transfer rate for SA in solution found in time-resolved fluorescence up-conversion measurements is 50 fs,[19] an atypically fast time scale for this process that usually occurs in a few picoseconds.[1,20] The comparison of the rate transfer processes for protium and deuterium reveals the absence of tunneling effects for ESIPT in SA.[19] Concerning computational studies, there are also theoretical calculations that yield the energetic profile for the tautomerism of salicylideneaniline along the O-H distance in *i*) the ground (S_0) and *ii*) the first singlet excited (S_1) electronic states.[21,22] The potential energy curve in the S_1 state does not show an energetic barrier for the Schiff base to go from the enol to the keto isomer,[22] in consistency with the very fast ESIPT rate observed in SA (*vide infra*).

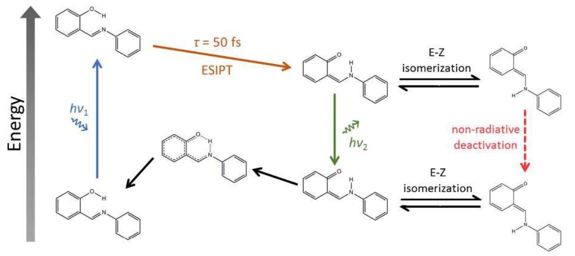

Scheme 1. Excited state intramolecular proton transfer within salicylideneaniline forming the keto tautomer. The subsequent relaxation to the ground state with the structure of the enol isomer is shown as well.

---

[a] Institute of Chemistry, National Autonomous University of México, Circuito Exterior, Ciudad Universitaria, Delegación Coyoacán C.P. 04510, México, D.F.
*To whom correspondence should be addressed tomasrocharinza@gmail.com

DOI: 10.1039/x0xx00000x

Despite the experimental and computational information about the ESIPT reactions[1,3–8,11,23–25] and especially that occurring in SA,[4,10,13,14,25,26] there are still unresolved issues to consider about this reaction. In particular, it is unclear which structural, electronic and bonding features are responsible for the proton transfer dynamics. Besides, some mechanistic studies of ESIPTs in colorants suggest that the migrating species could be either a proton or an electrically neutral hydrogen atom.[5,27] We investigated the reactivity in the ground and the first singlet excited states of SA by means of the Quantum Theory of Atoms in Molecules (QTAIM).[28] The nature of the transferred species in the ESIPT of SA was examined through the Laplacian of the electron density, $\nabla^2\rho(\mathbf{r})$, in both S_0 and S_1 electronic states. We decided to use quantum chemical topology (QCT) techniques because they have proven to offer valuable insights about photophysical[28] and photochemical[29] processes. In addition, QCT methods are particularly suitable for this investigation because electronically excited states have bond orders and other descriptors of the electronic structure of a molecule drastically altered in comparison with those in the electronic ground state. Such variations can be properly characterized by topological analyses such as QTAIM. More specifically, in this study it will be possible to relate changes in the aromaticity of a molecule after electron excitation to reaction dynamics in the first singlet excited state.

Concerning the electronic structure calculations performed in this work, the corresponding degree of freedom for the keto-enol tautomerism of salicylideneaniline in the electronic states S_0 and S_1 was the internuclear distance between the oxygen and the transferred hydrogen atom $d_{\text{O–H}}$ as shown in the bottom of Figure 1. Partial geometry optimizations in the aforementioned electronic states were performed for different values of $d_{\text{O–H}}$ to study the intramolecular transfer reaction of interest. We used density functional theory (DFT) and linear response time-dependent DFT for the computation of electronic energies and densities at the ground and the first singlet excited state respectively. The exchange-correlation functional τHCTH-hyb[30] along with the 6-311G++(d,p) basis set were considered throughout this work, because their joint utilization has provided a good description of excited electronic states in organic molecules.[28] The choice of this functional was also based on the fact that it describes very well the emission and absorption of SA in cyclohexane, which are the experimental values taken as reference (Table S1 in the Supporting Information). The results obtained with τHCTH-hyb are to be contrasted with those computed with range separated-functionals like CAM-B3LYP[31] and LC-BLYP[32] which have considerably large errors (up to 0.79 and 0.74 eV for the absorption and emission respectively) with respect to the experimental value.

The Gaussian 09 package[33] was used for all electronic structure calculations. The ground and excited state QTAIM analysis was done as recently suggested in reference 28. More precisely, atomic energies were calculated by considering the virial ratio and the Kohn-Sham noninteracting kinetic energy.[28] The examination of the QTAIM properties and $\nabla^2\rho(\mathbf{r})$ for the ground S_0 and the excited state S_1 was performed using the AIMAll package.[34]

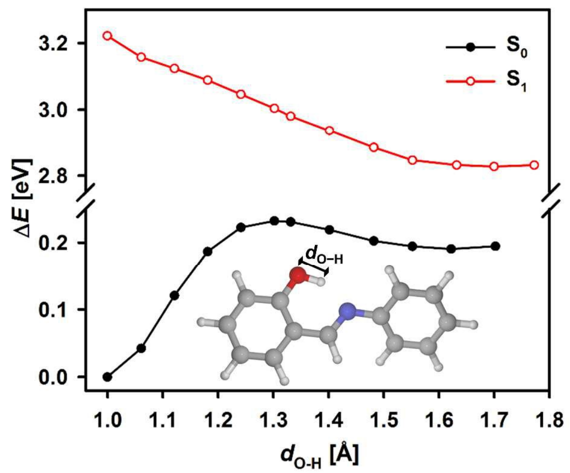

Figure 1. Potential energy curves for the conversion from the enol to the keto tautomer in the S_0 and S_1 states of salicylideneaniline.

We first consider the potential energy curves for the prototropic tautomerism of salicylideneaniline in the S_0 and S_1 states as shown in Figure 1. The results agree with those from Ortiz-Sánchez *et al.*,[22] thereby indicating the suitability of the exchange-correlation functional and basis set considered in this study. Similar profiles to those observed in Figure 1 were calculated with the aid of the long range corrected functionals CAM-B3LYP and LC-BLYP (Figure S1 on the Supporting Information), with the aforementioned difference that the τHCTH-hyb approximation compares better with experiment regarding the absorption and emission of SA. Concerning the ground state (black curve in Figure 1) the reaction involves an energetic barrier of 0.23 eV = 5.36 kcal/mol which prevents the occurrence of a fast proton transfer in S_0. The structure of the corresponding transition state has an oxygen-hydrogen distance $d_{\text{O–H}}$ = 1.3 Å. The energy profile changes radically in the first singlet excited state as shown in the red profile in Figure 1 wherein the reaction from the enol to the keto tautomer in the S_1 state is a barrierless process. The computed energy profile is in accordance with the very fast rate of ESIPT in SA.[19]

The electron density analysis presented in this article relies on the division of salicylideneaniline into the following groups: (a) the atoms participating directly in the tautomerism reaction: *i*) the oxygen, *ii*) the nitrogen and *iii*) the transferred H indicated as H*; (b) the aromatic rings: *iv*) $-C_6H_5$ (aniline ring) and *v*) $-C_6H_4$ (phenol cycle); and (c) *vi*) the −CH group as shown in Scheme 2(a). This partition is based on the different role that each group might have in the resonance assisted hydrogen bond (RAHB) entailed in the tautomerism of salicylideneaniline (Scheme 2(b)).

We consider now the change in group energies, $\Delta E(A)$, which fulfil the relationship

$$\Delta E = \sum_A \Delta E(A), \tag{1}$$

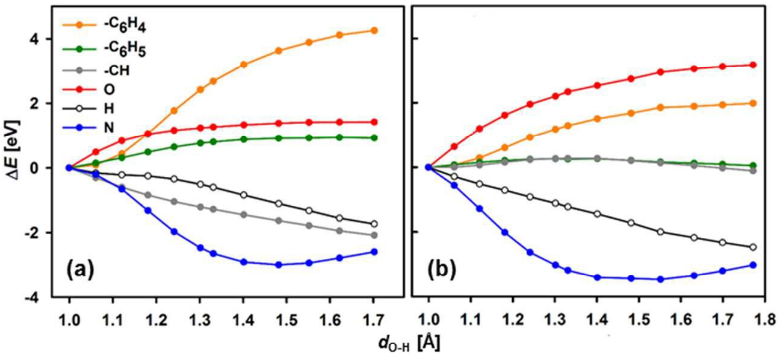

Figure 2. Change in the energies of the groups displayed in the first part of Scheme 2 in (a) the ground and (b) the first singlet excited state in the conversion from the enol to the keto tautomer of salicylideneaniline.

in which ΔE is the change of energy associated to a given process. Figures 2(a) and (b) show the changes of the group energies (Scheme 2(a)) throughout the conversion from the enol to the keto structure. We note that the groups $-C_6H_4$ and O (N and H*) become destabilized (stabilized) in both the ground and first singlet excited state. It is the reduction of energy of the N and H* groups which allows the reaction to occur in the S_1 state.

In order to further compare the changes of the group energies across the transformation from the enol into the keto isomer of SA, we considered the difference in the values of ΔE for the reaction in the ground and the first singlet excited state, $\Delta\Delta E$, together with the corresponding group contributions,

$$\Delta\Delta E = \Delta E(S_1) - \Delta E(S_0) = \sum_A \Delta\Delta E(A) = \sum_A \big(\Delta E(A,S_1) - \Delta E(A,S_0)\big). \tag{2}$$

where $\Delta E(S_1)$ ($\Delta E(S_0)$) is the change in energy of the enol to the keto isomers transformation in the S_1 (S_0) state, and $\Delta E(A,S_1)$ ($\Delta E(A,S_0)$) is the corresponding contribution from group A. The more negative the value of $\Delta\Delta E(A)$, the larger the contribution of A to the observed difference in reactivity of the S_0 and S_1 states in the intramolecular hydrogen transfer of SA. Table 1 points out that the most important negative contributions to $\Delta\Delta E$ come from the aromatic rings within SA. Figure 2(b) and Table 1 show that even when $\Delta E(-C_6H_4, S_1) = 1.99$ eV > 0, the value of $\Delta\Delta E(-C_6H_4)$ is negative (−2.18 eV). This means that the electron redistribution represented in Scheme 2(b) increases the energy of the $-C_6H_4$ group across the transformation from the enol to the keto structure in both S_0 and S_1 electronic states, but the increment is considerably smaller in the latter case.

The increase of the $-C_6H_4$ energy in the enol to keto tautomerism of SA is consistent with the fact that this reaction destroys the aromatic sextet of this cyclic structure as seen in the right of Scheme 1. Hence, we decided to investigate the aromatic character in both electronic states of the phenol ring by means of the index[35]

$$\theta'(\Omega) = \left(\sum_{A\in\Omega} (\delta_A - \delta_0)^2\right)^{\frac{1}{2}}, \tag{3}$$

in which δ_0 is the sum of electron delocalization of a carbon in the benzene molecule in its ground state while δ_A is the comparable quantity of a C atom within a particular ring, e.g. the $-C_6H_4$ unit. The parameter θ' measures the deviation between the uniform electron delocalization of C_6H_6 in its S_0 state and that found in a specific cyclic structure. The aromatic character of a given ring is reduced with increasing values of θ'. Figure 3 shows the evolution of θ' throughout the reaction for the $-C_6H_4$ cycle for the two electronic states under consideration. As expected, the aromaticity of the phenol moiety is lost as the reaction proceeds. Although the delocalization indices of the keto form in the S_0 and S_1 states differ considerably (the RMSD deviation being 0.46 which is higher than any value of $\theta'(\Omega)$ in Figure 3), the aromaticity of the S_0 and S_1 states of the keto form of SA are similar as indicated by $\theta'(\Omega)$. This statement is also supported by the multicentre aromaticity indices $I_{\mathrm{Ring}}(\Omega)$,[36] $I_{\mathrm{NG}}(\Omega)$,[37] $\mathrm{MCI}(\Omega)$,[38] and $I_{\mathrm{NB}}(\Omega)$[37] (assessed in reference 39 for the analysis of chemical reactions) as shown in Figure S2. As opposed to the

Table 1. Values of $\Delta\Delta E$ (Equation (2)) for the groups of Scheme 2(a) in the transformation from the enol to the keto form of salicylideneaniline.

Group	$\Delta\Delta E$ /eV	Group	$\Delta\Delta E$ /eV
$-C_6H_4$	−2.176	H*	−0.770
$-C_6H_5$	−0.848	N	−0.424
CH	1.922	O	1.709
Total	−0.588		

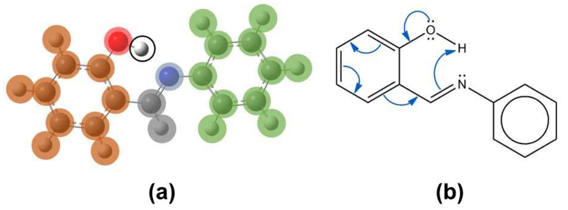

Scheme 2 (a) Partition of the salicylideneaniline molecule considered in this work. (b) Resonance assisted hydrogen bond involved in the proton transfer in ground and excited states of salicylideneaniline.

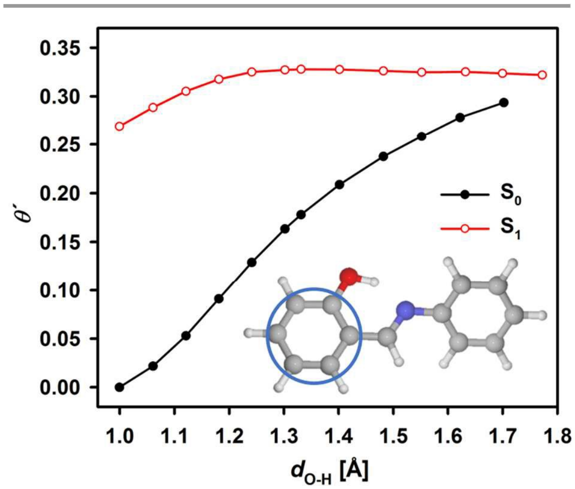

Figure 3. Aromaticity index θ', equation (3), for the $–C_6H_4$ ring across the transformation from the enol to the keto isomer of salicylideneaniline in the S_0 and S_1 states.

aromaticity index $\theta'(\Omega)$, the aromatic character of a given ring Ω increases with the values of $I_{\mathrm{Ring}}(\Omega)$, $I_{\mathrm{NG}}(\Omega)$, MCI(Ω), and $I_{\mathrm{NB}}(\Omega)$. The indices $I_{\mathrm{Ring}}(\Omega)$ and $I_{\mathrm{NG}}(\Omega)$ predict even that the aromatic character of keto isomer in the first singlet excited state is larger than it is in S_0. In addition, the curve for the former state is far steeper than that of the latter. Indeed, the enol tautomer is significantly less aromatic in the S_1 state than it is in S_0. This means that the absorption of light triggering the reaction substantially impairs the aromaticity of the phenol structure, and thereby propels the tautomerism of SA in the excited state. Because the aromatic character of the $–C_6H_4$ moiety has already been weakened as a consequence of electron excitation, the energetic change of this functional group as the S_1 tautomerization takes place does not overwhelm the stabilization of the N and H* atoms during the reaction. The electron redistribution associated to the RAHB described in Scheme 2(b) occurs without a barrier, leading to the enol-keto taumerism of SA in the S_1 state. On the contrary, the loss of aromaticity of the $–C_6H_4$ ring in ground state is prohibitive for the reaction to occur as reflected in the very large increase of the energy of this group in Figure 2(a) (4.26 eV). We obtained a similar description of the driving force of the ESIPT of SA through the use of the multicentre indices in Figure S2. The fact that the $I_{\mathrm{Ring}}(\Omega)$ and $I_{\mathrm{NG}}(\Omega)$ indicator predict a larger aromaticity for the keto form in the first singlet excited state than for S_0 provides further evidence that the loss in aromaticity throughout the tautomerization reaction in ground state is far more prohibitive than it is in the S_1 state as stated above. Although the aromaticity of the $–C_6H_5$ group is reduced after photoexcitation, the changes in the aromatic character of the aniline ring are smaller than those of the phenol moiety in virtue that the aromatic sextet of the former is not destroyed throughout the tautomerism reaction.

Finally, to determine the nature of the transferred species (i.e. whether it is a proton or a neutral hydrogen atom) in the reaction under study, we considered the QTAIM populations of H* throughout the potential energy curve of the first singlet excited state in Figure 1 (red profile). A bare proton (neutral hydrogen atom) will have an atomic population close to zero (one) electrons. Figure 4(a) shows that the atomic population of H* across the prototropism of SA in S_0 and S_1 is intermediate between these two limit situations. The number of electrons in H* across the hydrogen atom transfer reaction goes from 0.4 to 0.5 in both electronic states. This might be related to the difficulty to experimentally determine the character of the conveyed hydrogen atom. On one hand laser flash photolysis[27] and time resolved luminescence[15] experiments indicate the transfer of a neutral hydrogen atom while on the other time-resolved photoelectron spectroscopy[10] points to the transfer of a proton.

To further examine the character of the transferred hydrogen atom, we considered profiles of $\nabla^2\rho(\mathbf{r})$ across the prototropism reaction shown in Figure 4(b). It is observed that there is a region of local charge concentration connecting the basins of the oxygen, hydrogen and nitrogen atoms involved in the reaction in the excited state S_1. We compared these profiles with those corresponding to the systems $[F\cdots H\cdots F]^-$ and $[H_3C\cdots H\cdots CH_3]^{\cdot}$ (Figures 4(c) and (d)) the intermediate species in the transfer of *i*) H^+ between HF and F^- and *ii*) $H^{\cdot}$ amidst $H_3C^{\cdot}$ and CH_4. As Figure 4(b) illustrates, the profiles for $\nabla^2\rho(\mathbf{r})$ in the ESIPT of SA are similar to those for the transfer of a neutral hydrogen atom in the reaction $H_3C^{\cdot} + H_4C \rightarrow H_3C\text{-}H + {}^{\cdot}CH_3$ (Figure 4(d)) and differ considerably to those for the proton transfer in Figure 4(c) wherein the regions separating the hydrogen from the fluorine atoms are characterized by a local depletion of electron charge. Thus, in consistency with the population analysis discussed above, the contours of $\nabla^2\rho(\mathbf{r})$ indicate that there is an important amount of electron distribution around the hydrogen atom transferred in the tautomerism of SA under investigation. To finish this communication, we indicate that similar interpretations about the ultrafast ESIPT reaction of SA based on the topology of the electron density, its Laplacian and aromaticity indices are obtained by using the long range corrected CAM-B3LYP functional along with the same basis set used up to this point as shown in figures S3-S6 and Table S2 on the Supporting

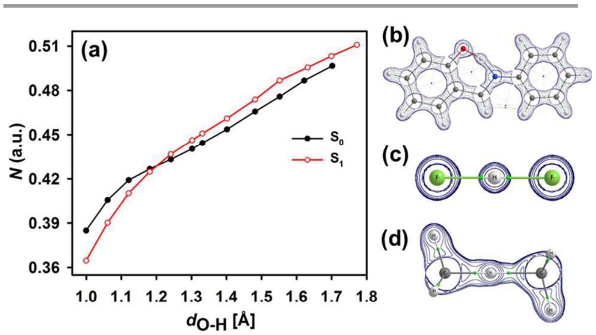

Figure 4. (a) Changes of the atom population of H* throughout the prototropism of salicylideneaniline in the S_0 and S_1 states. Profiles of $\nabla^2\rho(\mathbf{r})$ in the midpoint of the atom hydrogen transfer within (b) salicylideneaniline in its first singlet excited state along with those in the ground state between (c) $F^- + HF$ and (d) $CH_4 + CH_3^{\cdot}$.

Information.

Conclusions

We studied the driving force and the nature of the conveyed species in the ESIPT of salicylideneaniline through quantum chemical topology analyses. The results indicate that the marked differences in ESIPT reactivity for the S_0 and S_1 states of salicylideneaniline are due to a considerable loss in aromaticity after photoexcitation, allowing thereby the redistribution of electron density to trigger the tautomerization reaction. Additionally, the analyses of atomic populations along with that of the Laplacian of the electron distribution indicate that the reaction involves the transfer of a hydrogen atom associated with an amount of charge density intermediate between that in a bare proton and a neutral hydrogen atom. Overall, we show how the analysis provided in this communication by means of quantum chemical topology methods might help in the understanding of ESIPT reactions, especially about the driving force of the process and the nature of the transferred species. In particular, we have herein done the first quantitative description of how the electronic structure changes that occur upon electronic excitation propel a photochemical process. We anticipate that this kind of investigation will yield valuable insights on other reactions of interest to the photochemistry community.

Acknowledgements

The authors gratefully acknowledge CONACyT-México (project 220392 and Ph.D. scholarship 257981) and PAPIIT/DGAPA/UNAM (grant IN209715) for financial support along with DGTIC/UNAM (projects SC15-1-IG-36, SC15-1-S-73 and SC15-1-MP-62) for computer time.

References

1 J. Zhao, S. Ji, Y. Chen, H. Guo and P. Yang, *Phys. Chem. Chem. Phys.*, 2012, **14**, 8803.
2 A. O. Doroshenko, A. Y. Matsakov, O. V. Nevskii and O. V. Grygorovych, *J. Photochem. Photobiol. A Chem.*, 2012, **250**, 40–49.
3 F. Gao, X. Wang, H. Li and X. Ye, *Tetrahedron*, 2013, **69**, 5355–5366.
4 S. Mitra, A. K. Chandra, P. M. Gashnga, S. Jenkins and S. R. Kirk, *J. Mol. Model.*, 2012, **18**, 4225–4237.
5 V. Vetokhina, K. Dobek, M. Kijak, I. I. Kamińska, K. Muller, W. R. Thiel, J. Waluk and J. Herbich, *ChemPhysChem*, 2012, **13**, 3661–3671.
6 T. Y. Lin, K. C. Tang, S. H. Yang, J. Y. Shen, Y. M. Cheng, H. A. Pan, Y. Chi and P. T. Chou, *J. Phys. Chem. A*, 2012, **116**, 4438–4444.
7 N. Singla and P. Chowdhury, *Chem. Phys. Lett.*, 2012, **548**, 71–79.
8 P. Wnuk, G. Burdzinski, M. Sliwa, M. Kijak, A. Grabowska, J. Sepiol and J. Kubicki, *Phys. Chem. Chem. Phys.*, 2014, **16**, 2542–2552.
9 W. C. Lin, S. K. Fang, J. W. Hu, H. Y. Tsai and K. Y. Chen, *Anal. Chem.*, 2014, **86**, 4648–4652.
10 T. Sekikawa, O. Schalk, G. Wu, a. E. Boguslavskiy and a. Stolow, *Springer Proc. Phys.*, 2012, **125**, 313–315.
11 J. E. Kwon and S. Y. Park, *Adv. Mater.*, 2011, **23**, 3615–3642.
12 A. Samanta, S. Dalapati and N. Guchhait, *J. Photochem. Photobiol. A Chem.*, 2012, **232**, 64–72.
13 J. Jankowska, J. Sadlej and A. L. Sobolewski, *Phys. Chem. Chem. Phys.*, 2015, **17**, 14484–14488.
14 V. C. Víctor, *J. Phys. Chem. A*, 2004, **108**, 281–288.
15 T. Kobayashi, T. Sekikawa and T. Inabe, *J. Lumin.*, 1997, **72-74**, 508–510.
16 T. C. Fang, H. Y. Tsai, M. H. Luo, C. W. Chang and K. Y. Chen, *Chinese Chem. Lett.*, 2013, **24**, 145–148.
17 A. J. Moghadam, R. Omidyan and V. Mirkhani, *Phys. Chem. Chem. Phys.*, 2014, **16**, 2417–24.
18 C. Randino, M. Ziółek, R. Gelabert, J. A. Organero, M. Gil, M. Moreno, J. M. Lluch and A. Douhal, *Phys. Chem. Chem. Phys.*, 2011, **13**, 14960–14972.
19 W. Rodríguez-Córdoba, J. S. Zugazagoitia, E. Collado-Fregoso and J. Peon, *J. Phys. Chem. A*, 2007, **111**, 6241–6247.
20 F. Gao, X. Zhong, Q. Wang, H. Li and S. Zhang, *Chinese J. Chem.*, 2010, **28**, 1057–1068.
21 J. M. Ortiz-Sanchez, R. Gelabert, M. Moreno and J. M. Lluch, *J. Phys. Chem. A*, 2006, **110**, 4649–4656.
22 J. M. Ortiz-Sánchez, R. Gelabert, M. Moreno and J. M. Lluch, *J. Chem. Phys.*, 2008, **129**, 1–12.
23 Y. Shigemitsu, T. Mutai, H. Houjou and K. Araki, *J. Phys. Chem. A*, 2012, **116**, 12041–12048.
24 S. Hayaki, Y. Kimura and H. Sato, *J. Phys. Chem. B*, 2013, **117**, 6759–6767.
25 S. Mitra and N. Tamai, *Chem. Phys. Lett.*, 1998, **282**, 391–397.
26 S. Mitra and N. Tamai, *Phys. Chem. Chem. Phys.*, 2003, **5**, 4647.
27 S V Jovanovic, S. Steenken, C. W. Boone and M. G. Simic, *J. Am. Chem. Soc.*, 1999, **121**, 9677–9681.
28 E. I. Sánchez-Flores, R. Chávez-Calvillo, T. A. Keith, G. Cuevas, T. Rocha-Rinza and F. Cortés-Guzmán, *J. Comput. Chem.*, 2014, **35**, 820–828.
29 L. Gutiérrez-Arzaluz, T. Rocha-Rinza and F. Cortés-Guzmán, *Comput. Theor. Chem.*, 2015, **1053**, 214–219.
30 A. D. Boese and N. C. Handy, *J. Chem. Phys.*, 2002, **116**, 9559.
31 T. Yanai, D. P. Tew and N. C. Handy, *Chem. Phys. Lett.*, 2004, **393**, 51–57.
32 H. Iikura, T. Tsuneda, T. Yanai and K. Hirao, *J. Chem. Phys.*, 2001, **115**.
33 M. J. Frisch, G. W. Trucks, H. B. Schlegel, G. E. Scuseria, M. A. Robb, J. R. Cheeseman, G. Scalmani, V. Barone, B. Mennucci, G. A. Petersson, et al., *Gaussian 09* (*revision D.01*), Gaussian Inc., Wallingford, CT, 2009.
34 T. A. Keith, *AIMAll*, *version 14.06.21*, TK Gristmill Software, Overland Park, KS, 2015.
35 M. Garcia-Revilla and J. Hernandez-Trujillo, *Phys. Chem. Chem. Phys.*, 2009, **11**, 8425–8432.
36 M. Giambiagi, M. S. de Giambiagi, C. D. dos Santos Silva and A. P. de Figueiredo, *Phys. Chem. Chem. Phys.*, 2000, **2**, 3381–3392.
37 J. Cioslowski, E. Matito and M. Solà, *J. Phys. Chem. A*, 2007, **111**, 6521–6525.
38 P. Bultinck, M. Rafat, R. Ponec, B. Van Gheluwe, R. Carbó-Dorca and P. Popelier, *J. Phys. Chem. A*, 2006, **110**, 7642–7648.
39 F. Feixas, E. Matito, J. Poater and M. Solà, *J. Comput. Chem.*, 2008, **29**, 1543–1554.